J|A|C|S
ARTICLES
Published on Web 07/13/2002

The Dean−Evans Relation in ^{31}P NMR Spectroscopy and Its Application to the Chemistry of Octahedral Tungsten Sulfide Clusters

Song Jin, Jennifer Adamchuk, Bosong Xiang, and Francis J. DiSalvo*

Contribution from Baker Laboratory, Department of Chemistry and Chemical Biology, Cornell University, Ithaca, New York 14853

Received February 1, 2002

Abstract: One of the challenges in studying the chemistry of hexanuclear octahedral metal clusters is analyzing the many possible complexes, including stereoisomers, when these complexes consist of mixed axial ligands (two or more). In the case of $W_6S_8L_{6-n}(PR_3)_n$ ($n = 0-6$; L = nonphosphine Lewis base ligands, PR_3 = phosphines) clusters, in situ identification of the 10 possible complexes is possible by ^{31}P NMR due to P−W−W−P coupling. A linear relation for ^{31}P NMR shifts ($\delta(^{31}P)$) of these $W_6S_8L_{6-n}(PR_3)_n$ complexes, analogous to the Dean−Evans relation for ^{19}F NMR shifts of octahedral tin complexes, is found and expressed as $\delta(^{31}P) = \delta_{ref} + pC + qT$ with two variables (p and q, the number of ligands L in the cis or trans position to PR_3, respectively) with two constants (C and T, characteristic of a given ligand L). ^{31}P NMR investigation of over 200 complexes in 26 $W_6S_8L_{6-n}(PR_3)_n$ systems show that this relation is generally valid for W_6S_8 clusters. Such a relation helps spectroscopic assignments and demonstrates the trans and cis influence on hexanuclear clusters. Large bulky ligands cause deviations from the linear behavior due to steric effects. With the help of 2-D ^{31}P NMR spectroscopy, mixtures of $W_6S_8(PR_3)_{6-n}(PR'_3)_n$ ($n = 0-6$) complexes can also be unequivocally interpreted. The Dean−Evans relation is expanded to account for different phosphine ligands. Partial substitution reactions of these W_6S_8 complexes by phosphines were investigated using ^{31}P NMR, and four single crystals of mixed-ligand clusters are characterized with X-ray diffraction. In summary, ^{31}P NMR and other NMR techniques, combined with Dean−Evans relations, are invaluable analytical tools for studying molecular W_6S_8 cluster chemistry and are likely to be useful for studying other mixed-ligand metal clusters.

Introduction

The chemistry of molecular hexanuclear metal clusters has come a long way since the early crystallographic studies in the 1940s.[1] The two main structural units of these clusters are based on face or edge capping of a metal octahedron by anions (M_6X_8 and M_6X_{12}, respectively).[2−9] Each metal atom of the octahedron is able to bind an electron donor, resulting in an *octahedral* configuration for these outer (axial) ligands. A coordination chemistry parallel to that of the classical Werner type *octahedral metal complexes* was envisioned for such *octahedral clusters* as early as the 1960s.[5,10] However, with some notable exceptions of clusters with two[11−15] or more[16] kinds of ligands, such development has yet to become a reality, partially because of the analytical challenges presented by the large number of possible complexes. With just 2 ligands, 10 different possible complexes, including 3 pairs of stereoisomers, result from stepwise substitution on octahedral complexes. As observed by other researchers in the field, the nearly exclusive reliance on crystallography and the lack of convenient and sensitive

* To whom correspondence should be addressed. E-mail: fjd3@cornell.edu.

(1) Brosset, C. *Ark. Kem., Mineral. Geol.* **1945**, *A20*, 16; Brosset, C. *Ark. Kem., Mineral. Geol.* **1946**, *A22*, 10. Vaughan, P. A.; Sturdivant, J. H.; Pauling, L. *J. Am. Chem. Soc.* **1950**, *72*, 5477−5486. Vaughan, P. A. *Proc. Natl. Acad. Sci. U.S.A.* **1950**, *36*, 461−464.
(2) Ziebarth, R. P.; Corbett, J. D. *Acc. Chem. Res.* **1989**, *22*, 256−262.
(3) Lee, S. C.; Holm, R. H. *Angew. Chem.* **1990**, *102*, 868−885.
(4) Corbett, J. D. *J. Alloys Compd.* **1995**, *229*, 10−23.
(5) Preetz, W.; Peters, G.; Bublitz, D. *Chem. Rev.* **1996**, *96*, 977−1025.
(6) Saito, T. *Adv. Inorg. Chem.* **1997**, *44*, 45−91.
(7) Prokopuk, N.; Shriver, D. F. *Adv. Inorg. Chem.* **1998**, *46*, 1−49.
(8) Saito, T. *J. Chem. Soc., Dalton Trans.* **1999**, 97−106.
(9) Gabriel, J.-C. P.; Boubekeur, K.; Uriel, S.; Batail, P. *Chem. Rev.* **2001**, *101*, 2037−2066.
(10) Penfold, B. R. *Perspect. Struct. Chem.* **1968**, *2*, 71−149.
(11) Saito, T.; Nishida, M.; Yamagata, T.; Yamagata, Y.; Yamaguchi, Y. *Inorg. Chem.* **1986**, *25*, 1111−1117. Schaefer, H.; Brendel, C.; Henkel, G.; Krebs, B. *Z. Anorg. Allg. Chem.* **1982**, *491*, 275−285. Perchenek, N.; Simon, A. *Z. Anorg. Allg. Chem.* **1993**, *619*, 98−102. Ehrlich, G. M.; Deng, H.; Hill, L. I.; Steigerwald, M. L.; Squattrito, P. J.; DiSalvo, F. J. *Inorg. Chem.* **1995**, *34*, 2480−2482.
(12) Zheng, Z.; Long, J. R.; Holm, R. H. *J. Am. Chem. Soc.* **1997**, *119*, 2163-2171. Zheng, Z.; Holm, R. H. *Inorg. Chem.* **1997**, *36*, 5173−5178. Willer, M. W.; Long, J. R.; McLauchlan, C. C.; Holm, R. H. *Inorg. Chem.* **1998**, *37*, 328−333. Zheng, Z.; Gray, T. G.; Holm, R. H. *Inorg. Chem.* **1999**, *38*, 4888−4895. Selby, H. D.; Zheng, Z.; Gray, T. G.; Holm, R. H. *Inorg. Chim. Acta* **2001**, *312*, 205−209.
(13) Xie, X.; Reibenspies, J. H.; Hughbanks, T. *J. Am. Chem. Soc.* **1998**, *120*, 11391−11400. Harris, J. D.; Hughbanks, T. *J. Am. Chem. Soc.* **1997**, *119*, 9449−9459.
(14) Yoshimura, T.; Umakoshi, K.; Sasaki, Y.; Sykes, A. G. *Inorg. Chem.* **1999**, *38*, 5557−5564. Yoshimura, T.; Umakoshi, K.; Sasaki, Y.; Ishizaka, S.; Kim, H.-B.; Kitamura, N. *Inorg. Chem.* **2000**, *39*, 1765−1772. Chen, Z.-N.; Yoshimura, T.; Abe, M.; Sasaki, Y.; Ishizaka, S.; Kim, H.-B.; Kitamura, N. *Angew. Chem., Int. Ed.* **2001**, *40*, 239−242. Chen, Z.-N.; Yoshimura, T.; Abe, M.; Tsuge, K.; Sasaki, Y.; Ishizaka, S.; Kim, H.-B.; Kitamura, N. *Chem. Eur. J.* **2001**, *7*, 4447−4455.
(15) Jin, S.; Venkataraman, D.; DiSalvo, F. J. *Inorg. Chem.* **2000**, *39*, 2747−2757.
(16) Saito, T.; Nishida, M.; Yamagata, T.; Yamagata, Y.; Yamaguchi, Y. *Inorg. Chem.* **1986**, *25*, 1111−1117. Yamagata, Y.; Okiyama, H.; Imoto, H.; Saito, T. *Acta Crystallogr., Sect. C* **1997**, *C53*, 859−862.

Chart 1

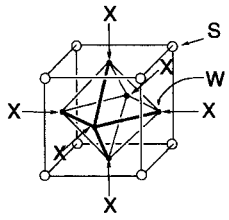

Schematic structure of a $W_6S_8(LL')_6$ cluster
X = PR_3 or L (non-phosphine Lewis base ligand)

Designation of the $W_6S_8L_{6-n}(PR_3)_n$ Cluster Series

L \ L'	PEt_3 **A**	P^nBu_3 **B**	PMe_3 **C**	PPh_3 **Y**	PCy_3 **Z**
*t*BuNC(**I**)	√	√	√		√
4-tbp(**II**)	√ *	√	√	√	√
piperidine(**III**)	√	√	√	√	√
n$BuNH_2$(**IV**)	√	√	√	√	√
t$BuNH_2$(**V**)	√	√	√		√
PEt_3 (**A**)	–	√ *			√ *

'√' indicates the series studied, L = bipy and PR_3 = PEt_3 was also studied. '*' indicates systems that were investigated with 2-D NMR. 4-tbp = 4-*tert*-butylpyridine.

analytical techniques[13] as well as separation techniques were all obstacles to the development of the solution chemistry of octahedral metal clusters.

We are particularly interested in the group VI octahedral metal chalcogenide clusters (M_6Q_8, M = Cr, Mo, W; Q = S, Se, Te; shown in Chart 1).[6] When M = Mo, these clusters are the building blocks of the famous Chevrel phases,[17] which were extensively studied for their superconductivity,[18] fast ionic conductivity,[19] thermoelectric properties,[20] and catalytic activity.[21] After the molecular $M_6Q_8L_6$ (L = organic Lewis base ligand) clusters were synthesized by Saito[22] and McCarley,[23] we focused on constructing novel solid-state materials using clusters dispersed in solution as building blocks. To that end, we studied the axial coordination chemistry of these clusters, particularly that of heteroleptic $W_6S_8L_{6-n}(PR_3)_n$ ($0 < n < 6$) clusters, in the hope of exploiting ligand binding strength differences to construct low-dimensional networks.[15] We were also faced with the problem of analyzing and identifying the 10 cluster complexes in the series. Fortunately, the ^{31}P NMR chemical shifts of these complexes are sufficiently separate and an unusual P−W−W−P coupling[15] enabled the identification of many of the 10 possible clusters. We also observed a linear relation in the ^{31}P NMR chemical shifts of these clusters, which is analogous to the Dean−Evans relation for the ^{19}F NMR chemical shifts of octahedral tin complexes.[24] As summarized in eq 1, the Dean−Evans relation can predict the chemical shifts of many $[SnX_{6-n}F_n]^{2-}$complexes in a rather simple and yet practically useful fashion:

$$\delta(^{19}F) = \delta_{ref} + pC + qT \qquad (1)$$

where $\delta(^{19}F)$ is the chemical shift of the F atom under consideration, δ_{ref} is the chemical shift of $[SnF_6]^{2-}$ referred to a standard, p is the number of X ligands in positions cis to F^- (0−4), q indicates the presence of the X ligand in the position trans to F^- (0 or 1), C and T are empirical constants characteristic for ligand X. This relation quantitatively elucidates the accumulative influences of the cis and trans substituents on the chemical shifts of the NMR nuclei under question.[5] The Dean−Evans relation has also been demonstrated for ^{19}F NMR of $\{[Mo_6Cl_8]X_{6-n}F_n\}^{2-}$ clusters.[5] Since we had found no reports of such linear relation for ^{31}P NMR chemical shifts, we initiated an NMR investigation, including 2-D NMR studies, of many cluster complexes (listed in Chart 1). We show that the Dean−Evans relations hold generally with some understandable exceptions. Combined with the P−P coupling, this newly discovered Dean−Evans relation enables instantaneous identification of many W_6S_8 clusters with phosphine ligands and therefore is a very useful tool in the study of octahedral cluster chemistry. The results of this investigation are reported in this article.

Experimental Section

General Considerations. The preparation and properties of $W_6S_8(4\text{-tbp})_6$ (4-tbp = 4-*tert*-butylpyridine) and related cluster complexes were reported previously.[25] The NMR solvent C_6D_6 (under N_2) was received from Cambridge Isotope Laboratories (CIL) and used without further treatment. All reagents and products were stored in a glovebox

(17) Chevrel, R.; Sergent, M.; Prigent, J. *J. Solid State Chem.* **1971**, *3*, 515−519.
(18) Chevrel, R.; Sergent, M. In *Topics in Current Physics*; Chevrel, R., Sergent, M., Eds.; Springer-Verlag: Heidelberg, Germany, 1982; Vol. 32, Chapter 2.
(19) Mulhern, P. J.; Haering, R. R. *Can. J. Phys.* **1984**, *62*, 527−531. Aurbach, D.; Lu, Z.; Schechter, A.; Gofer, Y.; Gizbar, H.; Turgeman, R.; Cohen, Y.; Moshkovich, M.; Levi, E. *Nature* **2000**, *407*, 724−727.
(20) Caillat, T.; Fleurial, J. P.; Snyder, G. J. *Solid State Sci.* **1999**, *1*, 535−544. Roche, C.; Pecheur, P.; Toussaint, G.; Jenny, A.; Scherrer, H.; Scherrer, S. *J. Phys.: Condens. Matter* **1998**, *10*, L333-L339.
(21) McCarty, K. F.; Anderegg, J. W.; Schrader, G. L. *J. Catal.* **1985**, *93*, 375−387. Kareem, S. A.; Miranda, R. *J. Mol. Catal.* **1989**, *53*, 275−283. Hilsenbeck, S. J.; McCarley, R. E.; Thompson, R. K.; Flanagan, L. C.; Schrader, G. L. *J. Mol. Catal. A: Chem.* **1997**, *122*, 13−24.
(22) Saito, T.; Yamamoto, N.; Yamagata, T.; Imoto, H. *J. Am. Chem. Soc.* **1988**, *110*, 1646−1647. Saito, T.; Yoshikawa, A.; Yamagata, T. *Inorg. Chem.* **1989**, *28*, 3588−3592. Saito, T.; Yamamoto, N.; Nagase, T.; Tsuboi, T.; Kobayashi, K.; Yamagata, T.; Imoto, H.; Unoura, K. *Inorg. Chem.* **1990**, *29*, 764−770.
(23) Hilsenbeck, S. J.; Young, V. G., Jr.; McCarley, R. E. *Inorg. Chem.* **1994**, *33*, 1822−1832. Zhang, X.; McCarley, R. E. *Inorg. Chem.* **1995**, *34*, 2678−2683.
(24) Dean, P. A. W.; Evans, D. F. *J. Chem. Soc. A* **1968**, 1154−1166.
(25) Venkataraman, D.; Rayburn, L. L.; Hill, L. I.; Jin, S.; Malik, A.-S.; Turneau, K. J.; DiSalvo, F. J. *Inorg. Chem.* **1999**, *38*, 828−830.

filled with argon. All operations were carried out in the glovebox unless otherwise stated.

Preparation of the NMR Solutions. Most $W_6S_8L_{6-n}(PR_3)_n$ cluster solutions listed in Chart 1 were prepared in situ in 5 mm threaded NMR tubes equipped with Teflon-lined septa (Kontes Glass Inc.). Three methods were employed. (1) For most cases, about 20 mg of $W_6S_8L_6$ (L = nonphosphine Lewis base ligands) and 2−4 equiv of the desired PR_3 ligands were sealed into NMR tubes together with 1 mL of C_6D_6. Then the NMR tubes were brought out of the glovebox and heated at 50−100 °C for at least 12 h to produce, in most cases, mixtures of the entire $W_6S_8L_{6-n}(PR_3)_n$ ($n = 0-6$) cluster series. (2) For the more stable $W_6S_8L_6$ complexes, an alternative method was directly loading roughly equal molar ratios of $W_6S_8L_6$ and $W_6S_8(PR_3)_6$ with a total mass of about 25 mg into the NMR tubes and heating the sealed tubes as mentioned above. (3) If the $W_6S_8L_6$ complex is not available, repeatedly reacting $W_6S_8(PR_3)_6$ with excess nonphosphine ligand L produced the desired $W_6S_8L_{6-n}(PR_3)_n$ mixtures.

Preparation of the Solutions for 2-D NMR Studies. The $W_6S_8L_{6-n}(L')_n$ systems that were investigated with 2-D NMR spectroscopy are noted with asterisks in the table accompanying Chart 1. For optimal signal-to-noise ratios, the highest concentrations of the sample solutions are desired. Therefore, much larger amounts (>100 mg total mass) of the clusters were reacted in sealed thick-walled glass vessels with solvent (>5 mL benzene) and reacted in similar ways as above. The reaction mixtures were not completely soluble at the beginning, but they always became dark red homogeneous solutions after the reactions. After removal of the solvent, saturated solutions were made with 1 mL of C_6D_6 and transferred into NMR tubes.

One-Dimensional (1-D) ^{31}P NMR Experiments. ^{31}P NMR spectra were obtained using a Varian VXR-400 or a Varian INOVA-400 NMR spectrometer at 162 MHz with ^{1}H decoupling. A capillary filled with 85% H_3PO_4 was used as external standard or $W_6S_8(PEt_3)_6$ was used as internal secondary standard (δ −16.97). Routine 1-D ^{31}P NMR spectra were acquired with pulse width (pw) of 5 (VXR-400) or 8 μs (INOVA-400) (pw90 = 14 and 17 μs, respectively) and acquisition times of 1.6−2.4 s for optimal sensitivity and resolution. Sufficient signal-to-noise ratios were often achieved with 200−1000 scans in less than 1 h.

Two-Dimensional (2-D) ^{31}P-*J*-Resolved NMR Experiment. All 2-D NMR spectra, including the ^{31}P-*J*-resolved and ^{31}P-COSY spectra described below, were acquired on the INOVA-400 spectrometer and processed using the computer program NMRPipe.[26a] The experiments were set to acquire the 2-D data in the magnitude mode. Zero filling was used to double the digital resolution in both dimensions. The T_1 relaxation times of the ^{31}P NMR signals were measured to be about 2.7 s using the standard method of the spectrometer (specific values available in Table S1 of the Supporting Information). The pulse sequence for the ^{31}P-*J*-resolved experiment was the same as that used for the ^{1}H-*J*-resolved experiment.[26b] The pre-pulse and acquisition times were 0.65−1 and 1−1.4 s, respectively. The scan widths in the direct dimension were set to cover the whole ^{31}P spectra. For the indirect dimension, the scan widths in Hz and number of FIDs (>30) were equal to obtain a digital resolution of 1 Hz.

Two-Dimensional (2-D) ^{31}P-COSY NMR Experiments. The long-range COSY pulse sequence[26c,d] was used for the ^{31}P-COSY experiments. The fixed delays (0.04−0.1 s) before and after the second pulse was optimized on the basis of the P−P *J*-coupling constants (2.4 Hz) to obtain maximal cross-peaks in the COSY spectra. The pre-pulse and acquisition times were 1.0 and 0.6 s, respectively. The equal scan widths in both dimensions covered the entire ^{31}P chemical shift ranges of the specific samples. The number of FIDs for the indirect dimension were 256 and 512.

Statistical Analysis. Least-squares regression analyses were performed on the chemical shift data from the 1-D NMR spectra using the program included in SigmaPlot 2000 software packages.[27] An equation of the form $f = z0 + a*x + b*y$ was fit where f is the chemical shift ($\delta(^{31}P)$), $z0$ is the reference chemical shift (δ_{ref}), x and y are free variables (p and q), a and b are the fitted coefficients (C and T). The analysis of variance (AVONA) was also performed by the program but not reported herein for brevity. This and other details of the analyses are included in the reports of the Sigma Plot files available as Supporting Information.

Isolation Attempts by Differential Solvation and Chromatography. Large-scale mixtures of $W_6S_8(4\text{-tbp})_{6-n}(PEt_3)_n$ complexes were prepared by reacting $W_6S_8(4\text{-tbp})_6$[25] with 3 equiv of PEt_3 in benzene and divided into several portions. After the removal of solvent, many different solvents, including THF, dichloromethane, diethyl ether, acetonitrile, heptane, hexane, etc., were used to extract the solid residue. The resulting filtrates were dried and analyzed with ^{31}P NMR spectroscopy. On the basis of these results, a second round of extractions with different solvents, such as diethyl ether, acetonitrile, and heptane, was performed with the extracts or residues of the first round and analyzed with ^{31}P NMR again. Both the raw mixtures and the extracts were chromatographed on silica gel thin-layer chromatography plates with various solvents. Toluene seemed to give the best elution results. Large-scale column chromatography on silica gel or Florisil with toluene always led to retention of a band at the top of the column or discoloration during the elution and the recovery of often trace amounts of cluster complexes. Only $W_6S_8(PEt_3)_6$ (if present at the beginning) seemed to elute with little difficulty.

X-ray Structure Determination. The single-crystal X-ray crystallographic analyses described in this report were obtained from mostly serendipitously discovered crystals from various reaction mixtures. The crystallization conditions are as follows.

$W_6S_8(4\text{-tbp})_5(PEt_3)\cdot 3C_6H_6$ (1). A solid mixture of $W_6S_8(4\text{-tbp})_{6-n}(PEt_3)_n$ complexes of about 100 mg was extracted with diethyl ether. After removal of the diethyl ether, the filtrate residue was extracted again with acetonitrile. The dried acetonitrile filtrate was dissolved into benzene. The whole mixture was shown by ^{31}P NMR to contain $W_6S_8(4\text{-tbp})_5(PEt_3)$, *cis*-$W_6S_8(4\text{-tbp})_4(PEt_3)_2$, and a trace amount of *trans*-$W_6S_8(4\text{-tbp})_4(PEt_3)_2$. This solution was layered with heptane to produce dark red block crystals together with a great deal of orange-red precipitate over 4 weeks. The well-shaped block crystals were analyzed.

***cis*-$W_6S_8(4\text{-tbp})_2(PEt_3)_4$ (2).** A solid mixture of $W_6S_8(4\text{-tbp})_{6-n}(PEt_3)_n$ complexes made by reacting $W_6S_8(4\text{-tbp})_6$ with 2 equiv of PEt_3 in benzene was extracted with diethyl ether. After removal of the diethyl ether, this solid residue was washed with a copious amount of acetonitrile and finally with heptane. After the filtered orange-red heptane solution was stored in a capped vial for 1 month, some dark red wedge-shaped crystals appeared on the wall of the container along with many more tiny particles at the bottom. Only the large crystals were analyzed, but the whole mixture was shown by ^{31}P NMR to contain *cis*-$W_6S_8(4\text{-tbp})_2(PEt_3)_4$, *fac*-$W_6S_8(4\text{-tbp})_3(PEt_3)_3$, and smaller amounts of *mer*-$W_6S_8(4\text{-tbp})_3(PEt_3)_3$ and $W_6S_8(4\text{-tbp})(PEt_3)_5$.

$W_6S_8(PEt_3)_5$(bipy) (3). After $W_6S_8(PEt_3)_6$[25] was reacted with a large excess (>100 equiv) of 4,4′-bipyridyl (bipy) in benzene at 100 °C for 1 day, the solvent was removed and the residue was extracted with diethyl ether. The wine red solution was stored in a loosely capped vial to produce a large amount of colorless crystals (bipy) and some dark red block crystals over three weeks. Only the dark red crystals were analyzed, but the solution was shown by NMR to contain mainly bipy, $W_6S_8(PEt_3)_5$(bipy), and a trace amount of $W_6S_8(PEt_3)_6$ and other clusters.

(26) (a) Delaglio, F.; Grzesiek, S.; Vuister, G. W.; Zhu, G.; Pfeifer, J.; Bax, A. *J. Biomol. NMR* **1995**, *6*, 277−293. (b) Braun, S.; Kalinowski, H.-O.; Berger, S. *150 and More Basic NMR Experiments*; Wiley-VCH: New York, 1998; p 347. (c) Reference 26b, p 356. (d) Bax, A.; Freeman, R. *J. Magn. Reson.* **1981**, *44*, 542−561.

(27) Sigma Plot 2000, version 6.0; SPSS Inc., 2000.

Table 1. Crystallographic Data for $W_6S_8(4\text{-tbp})_5(PEt_3)\cdot 3C_6H_6$ (**1**), *cis*-$W_6S_8(4\text{-tbp})_2(PEt_3)_4$ (**2**), $W_6S_8(PEt_3)_5(bipy)$ (**3**), and *mer*-$W_6S_8(PEt_3)_3(PCy_3)_3\cdot 2C_6D_6$ (**4**)[a]

	1	2	3	4
chem formula	$C_{68}H_{97}N_5PS_8W_6$	$C_{42}H_{86}N_2P_4S_8W_6$	$C_{40}H_{83}N_2P_5S_8W_6$	$C_{84}H_{156}P_6S_8W_6$
fw	2375.06	2102.59	2106.51	2711.49
space group	$P2_1/c$ (No. 14)	$P2_1/c$ (No. 14)	$P\bar{1}$ (No. 2)	$P\bar{1}$ (No. 2)
a, Å	16.1816(4)	15.8389(12)	12.024(3)	15.0562(10)
b, Å	15.9178(4)	19.4806(14)	21.356(5)	16.2762(10)
c, Å	29.4907(8)	20.0882(15)	25.107(5)	20.4880(13)
α, deg	90	90	112.39(2)	88.980(2)
β, deg	91.4768(10)	95.542(2)	92.58(2)	74.256(2)
γ, deg	90	90	90.68(3)	78.297(2)
V, Å^3	7593.6(3)	6169.3(8)	5952.0(24)	4728.2(5)
Z	4	4	4	2
ρ_{calcd}, g cm^{-3}	2.077	2.264	2.351	1.905
μ, cm^{-1}	93.35	115.46	119.93	75.88
R1[b] ($I > 2\sigma$/all)	0.0571/ 0.1579	0.0388/ 0.0669	0.0712/ 0.1705	0.0498/ 0.1227
wR2[c] ($I > 2\sigma$/all)	0.1122/ 0.1660	0.0769/ 0.0837	0.1480/ 0.1791	0.0780/ 0.1122

[a] With $\lambda = 0.710\ 73$ Å at 173 K. [b] $R_1 = \sum||F_o| - |F_c||/\sum|F_o|$. [c] $wR_2 = [\sum w(F_o^2 - F_c^2)^2/\sum w(F_o^2)^2]^{1/2}$.

***mer*-$W_6S_8(PEt_3)_3(PCy_3)_3\cdot 2C_6D_6$ (4).** A solution of $W_6S_8(PEt_3)_{6-n}(PCy_3)_n$ mixture for NMR investigation was made by heating 10 mg of $W_6S_8(PCy_3)_6$[15] with 2 equiv of PEt_3 with 1 mL of C_6D_6 in a sealed NMR tube at 100 °C for a day. After NMR experiments, the solution was stored in a loosely capped vial and allowed to evaporate over 3 weeks. Large greenish brown block-shaped crystals were visible together with more tiny brown-red particles. ^{31}P NMR showed the solution contained mainly *mer*-$W_6S_8(PEt_3)_3(PCy_3)_3$, smaller amounts of *fac*-$W_6S_8(PEt_3)_3(PCy_3)_3$ and *cis*-$W_6S_8(PEt_3)_2(PCy_3)_4$, and trace amounts of *cis*-$W_6S_8(PEt_3)_4(PCy_3)_2$.

The selected crystals were mounted on a thin plastic loop using polybutene oil and were immediately placed in a cold dinitrogen stream. Single-crystal X-ray diffraction data were collected on a Bruker SMART system with a CCD detector using Mo Kα radiation at 173 K. The cell constants were determined from more than 50 well-centered reflections. The data were integrated using SAINT Plus software,[28] and empirical absorption corrections were applied using SADABS program (*β* revision).[29] The space groups were determined on the basis of systematic absences, intensity statistics and the successful refinements of the structures. The structures were solved using SHELXS[30] with direct methods to reveal the positions of W and S atoms. Difference Fourier syntheses following the subsequent full-matrix least-squares refinements on F_o^2 with SHELXL software packages revealed the ligand atoms. Hydrogen atoms were assigned to the ideal positions and refined using a riding model. There was some disorder in the *tert*-butyl groups of the ligands in structures **1** and **2**. Some restraints were imposed on the ethyl groups of the triethylphosphine ligand in **1** and **3**, and these atoms still had large thermal parameters. All nonsolvent non-hydrogen atoms were refined anisotropically in **2** and **4**; only W and S atoms were refined anisotropically in **1** and **3**. All final refinements converged, and the residual electron densities were near the W atoms. The crystallographic data are collected in Table 1, and detailed information on structural refinements is available as Supporting Information.

Results and Discussion

The proposed NMR investigation is enabled by facile preparation of *complete* mixtures of these W_6S_8 complexes. This has become routine due to the improved synthesis of W_6S_8(4-*tert*-butylpyridine)$_6$[25] and our general knowledge about the thermodynamics and kinetics of the formation of $W_6S_8L_6$.[31] Reacting a new ligand (L′) with $W_6S_8L_6$ at varying stoichiometric ratios above the corresponding kinetic threshold temperatures almost always produced a complete series of the 10 heteroleptic clusters $W_6S_8L_{6-n}L'_n$ ($n = 0-6$) (see more discussion in section B):

$$W_6S_8L_6 + xL' \rightarrow W_6S_8L_{6-n}(L')_n + nL + (x-n)L' \ (n = 0-6) \quad (2)$$

Reactions that yielded an incomplete cluster series could be complemented by additional reactions at different stoichiometries. For the observation of 1-D NMR spectra, in situ reactions in NMR tubes sufficed, though for 2-D NMR experiments, larger scale reactions had to be carried out to prepare more concentrated NMR solutions.

The investigated systems are listed in the table of Chart 1 and denoted with a combination of (arbitrarily assigned) shorthand labels. For instance, *cis*-$W_6S_8(4\text{-tbp})_2(PEt_3)_4$ can be represented as *cis*-**IIA**4, since there are two 4-*tert*-butylpyridine (**II**) and four (4) triethylphosphine (**A**) ligands on the W_6S_8 cluster in a cis configuration. We will also refer to the $W_6S_8(4\text{-tbp})_{6-n}(PEt_3)_n$ complex series as cluster series **IIA**. For the general case of $W_6S_8L_{6-n}(PR_3)_n$ complexes, we use "*cis*-P*n*" and such. Despite the emphasis on NMR spectroscopy, these analytical toolkit building efforts enabled in situ observation of ligand substitutions in finer detail and provided convenient analytical techniques to monitor the separation of the cluster complexes. A brief discussion of this follows the NMR section. Finally, the single X-ray crystal structures that emerged as exceptional cases out of the hundreds of complexes are discussed.

A. NMR Spectroscopy of $W_6S_8L_{6-n}L'_n$ ($0 < n < 6$) Complexes. i. Full Assignments of ^{31}P NMR Peaks in Situ for $W_6S_8L_{6-n}(PR_3)_n$ Complexes. Any *complete* series of $W_6S_8L_{6-n}(PR_3)_n$ (L = nonphosphine Lewis base ligand, PR_3 = tertiary phosphine ligands, $n = 0-6$) cluster complexes contains 10 different complexes (including both terminal members) and 12 different ^{31}P NMR peaks, as shown in Figure 1A for cluster series **IIA**. Fortunately, these NMR signals are well-separated from each other, with few exceptions noted later. Due to the *J* coupling through the cluster core (P−W−W−P),[15] 3 out of these 10 complexes, *mer*-**IIA**3, *cis*-**IIA**4, and **IIA**5, can be uniquely identified on the basis of their characteristic splitting patterns and intensity ratios. Furthermore, the fine P−P coupling in the satellite peaks of another 3 complexes, **IIA**1, *cis*-**IIA**2, and *fac*-**IIA**3, leads to their assignments. This was discussed in detail previously[15] and is verified by the direct observation of P−P couplings in the 2-D NMR experiments described below. We will invoke such results directly throughout the discussion herein. Now, the unassigned complexes, *trans*-**IIA**2, *trans*-**IIA**4, and **A**6 ($W_6S_8L_6$ does not have a ^{31}P NMR signal), can be differentiated using mass balance of the ligands if the starting stoichiometry is accurately known. We can also use the progression of the complexes—if a phosphine ligand is added onto $W_6S_8L_6$, the **IIA**2 complexes are reasonably assumed to

(28) SAINT Plus, Software for the CCD Detector System; Bruker Analytical X-ray Systems, Madison, WI, 1999.
(29) Sheldrick, G. M. SADABS (used by Siemens CCD Diffractometers); Institute für Anorganische Chemie der Universität Göttingen, Göttingen, Germany, 1999.
(30) Sheldrick, G. M. SHELXL, version 5.10; Siemens Analytical X-ray Instruments Inc., Madison, WI, 1999.
(31) Jin, S.; Zhou, R.; Scheuer, E. M.; Adamchuk, J.; Rayburn, L. L.; DiSalvo, F. J. *Inorg. Chem.* **2001**, *40*, 2666−2674.

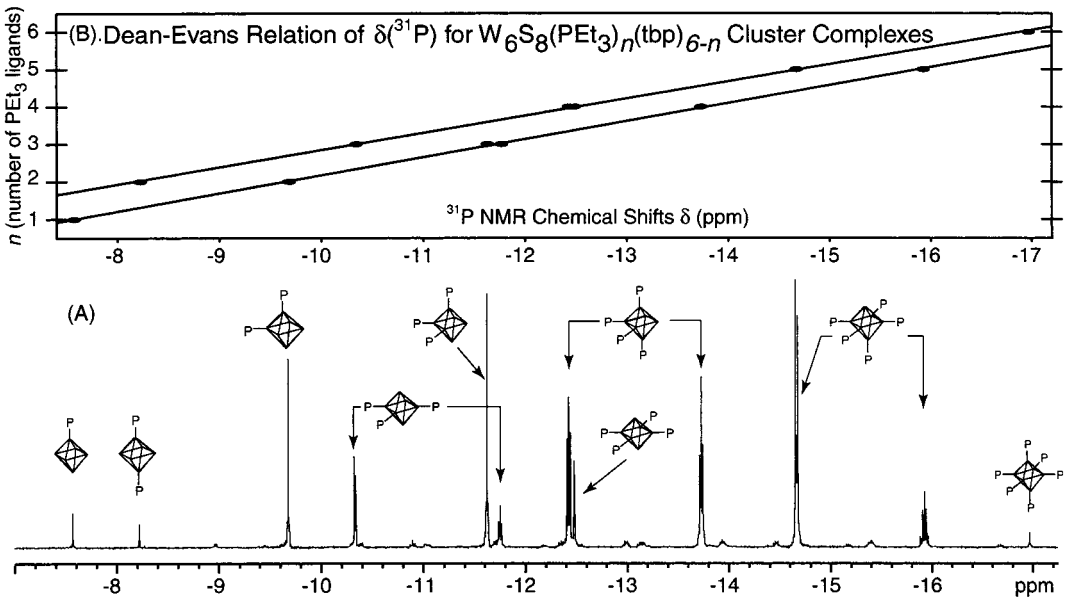

Figure 1. (A) ^{31}P{^{1}H} NMR spectrum for a mixture of $W_6S_8(4\text{-tbp})_{6-n}(PEt_3)_n$ ($n = 1-6$; **IIA**) cluster complexes. All main peaks are labeled; the satellite peaks are due to ^{183}W−P couplings and are discussed in ref 15. (B) Plot of the number of phosphine ligands (n) vs the assigned chemical shifts $\delta(^{31}P)$ (the Dean−Evans plot) for cluster series **IIA**.

emerge earlier than the **IIA**4 complexes during a slow reaction. In summary, every ^{31}P NMR signal from a mixture of $W_6S_8L_{6-n}(PR_3)_n$ complexes can be unambiguously assigned in situ with information only from ^{31}P NMR. Such an assignment is presented for series **IIA** in Figure 1A. The 1-D ^{31}P NMR spectra for all cluster systems studied were interpreted in a similar fashion, and the assigned chemical shifts are compiled in Table S2 in the Supporting Information.

ii. Dean-Evans Relation in the ^{31}P NMR Chemical Shifts of $W_6S_8L_{6-n}(PR_3)_n$ Complexes. With all NMR peaks assigned in Figure 1A, it is apparent that the chemical shifts of the **IIA** complexes progress from the left (downfield) to the right (upfield) of the NMR spectrum in a somewhat regular pattern with the stepwise addition of the phosphine ligand. Indeed, if the number of the phosphine ligands (n) is plotted against the corresponding chemical shifts, all data points appear to reside on two roughly parallel straight lines, as shown in Figure 1B (the upper panel). This linear relation in the ^{31}P NMR chemical shifts of $W_6S_8L_{6-n}(PR_3)_n$ complexes can be described in an equation analogous to the Dean-Evans relation:[24]

$$\delta(^{31}\mathrm{P}) = \delta_{\mathrm{ref}} + pC + qT \qquad (3)$$

where $\delta(^{31}P)$ is the chemical shift of the phosphorus atom in question, δ_{ref} is a reference chemical shift, q is the number of non-phosphine Lewis base ligands (L) in positions trans to the phosphine (PR_3) and is either 0 or 1, and p is the number of nonphosphine ligands (L) in positions cis to the phosphine and may take values from 0 to 4. C and T are empirical constants characteristic of ligand L corresponding to the influence of ligand L on $\delta(^{31}P)$ from the cis and trans positions, respectively. The trivial enumeration of the p and q values for each kind of phosphorus atom on an octahedron is listed in Table S2 of the Supporting Information. Regression analysis with the $\delta(^{31}P)$ values for cluster series **IIA** yielded $C = 2.13 \pm 0.02$ and $T = 0.80 \pm 0.06$ for L = 4-*tert*-butylpyridine with an excellent fit. Using these constants, two lines are also drawn in Figure 1B.

Table 2. *C* and *T* Constants (ppm) Determined for $W_6S_8L_{6-n}(PR_3)_n$ Complexes by Regression Analyses[a]

PR_3	L	C	T	r^2	$C-T$
PEt_3 (**A**)	*t*BuNC (**I**)	0.43 ± 0.02	−2.28 ± 0.06	0.994	2.72
	4-tbp (**II**)	2.13 ± 0.02	0.80 ± 0.06	0.999	1.33
	piperidine (**III**)	2.05 ± 0.03	1.40 ± 0.08	0.998	0.65
	*n*BuNH$_2$ (**IV**)	2.07 ± 0.04	1.59 ± 0.09	0.998	0.48
	*t*BuNH$_2$ (**V**)	2.39 ± 0.05	1.70 ± 0.12	0.997	0.69
	bipy	2.36 ± 0.05	0.47 ± 0.11	0.997	1.89
P^nBu_3 (**B**)	*t*BuNC (**I**)	0.74 ± 0.02	−1.98 ± 0.05	0.997	2.72
	4-tbp (**II**)	2.46 ± 0.04	0.65 ± 0.10	0.998	1.81
	piperidine (**III**)	2.17 ± 0.01	1.40 ± 0.04	0.9996	0.77
	*n*BuNH$_2$ (**IV**)	2.09 ± 0.03	1.63 ± 0.08	0.998	0.46
	*t*BuNH$_2$ (**V**)	2.30 ± 0.03	1.62 ± 0.06	0.999	0.69
PMe_3 (**C**)	4-tbp (**II**)	2.07 ± 0.07	0.70 ± 0.18	0.990	1.37
	piperidine (**III**)	1.94 ± 0.07	1.52 ± 0.18	0.989	0.42
	*n*BuNH$_2$ (**IV**)	1.99 ± 0.07	1.52 ± 0.18	0.989	0.47
	*t*BuNH$_2$ (**V**)	2.53 ± 0.09	1.78 ± 0.22	0.991	0.75

[a] Using the Dean−Evans relation $\delta(^{31}P) = \delta_{ref} + pC + qT$ as the function and Sigma Plot 2000 software. C and T values are followed by standard deviations.

It is noteworthy that the Dean−Evans relation does not use the number of phosphine ligands (n) as the free variable. Instead, two variables (p and q) are necessary for this empirical relation in order to differentiate the stereoisomers (when $n = 2-4$) and the two chemically inequivalent phosphorus atoms within one cluster complex (i.e. *mer*-P3, *cis*-P4, and P5). However, the "Dean−Evans graphs" are still plotted with n vs δ for convenience and historic consistency.[5]

iii. Generality of the Dean−Evans Relation in ^{31}P NMR and Its Implications. Fitting the observed chemical shifts with the Dean−Evans equation leads to remarkable success for the majority of the cluster series studied (the unsuccessful ones are discussed in part vi of this section). The C and T constants and the coefficients of determination (r^2) for the successful fittings are compiled in Table 2.

We include one more example of this spectrum interpretation and fitting process with cluster series **IB**, $W_6S_8(t\text{BuNC})_{6-n}(P^nBu_3)_n$. At first glance, the now familiar progressing pattern

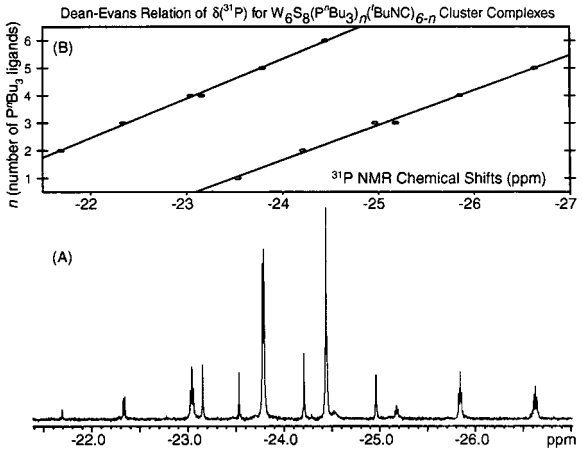

Figure 2. (A) $^{31}P\{^1H\}$ NMR spectrum for a mixture of $W_6S_8(^t\text{BuNC})_{6-n}(P^n\text{Bu}_3)_n$ ($n = 1-6$; **IB**) cluster complexes. (B) Plot of the number of phosphine ligands (n) vs the assigned chemical shifts $\delta(^{31}P)$ (the Dean−Evans plot) for cluster series **IB**.

of NMR peaks appears to be absent in the ^{31}P NMR spectrum of such a **IB** mixture, as shown in Figure 2A. However, a careful examination of the split peaks reveals three species, *mer*-3**IB** at δ −22.24 (doublet) and −25.18 (triplet), *cis*-4**IB** at −23.04 (triplet) and −25.84 (triplet), and 5**IB** at −23.79 (doublet) and −26.63 (quintet), which are evenly distributed in the spectrum from left to right. The anomaly is that the spans of each pair of those peaks (given by $C - T$) are so large that they overlap with one another. Fitting the assigned chemical shifts with the Dean−Evans relation is successful, as evidenced in the Dean−Evans plot in Figure 2B. Indeed, *t*BuNC in series **IB** has a negative T constant (-1.98 ± 0.05), as opposed to the positive values found for other ligands (see Table 2) so that $C - T > C$, making *t*BuNC ligand an unusual case. In the case of the $W_6S_8(t\text{BuNC})_{6-n}(PMe_3)_n$ series (**IC**), C and T constants are such that most NMR peaks are congested in a narrow region, making the peak assignments impossible without other information, such as 2-D NMR.

The examples raised above illustrate the utility of the Dean−Evans relation in assigning ^{31}P NMR shifts. Although solely relying on this relation to interpret NMR spectra may be a circular argument, a valid linear relation among the observed NMR shifts at the very least confirms the assignment of those uninformative singlets, such as *trans*-P2 and *trans*-P4, presuming its generality. Thus, the full assignment of NMR peaks in practice is often simpler than what is described in part i. One could even imagine using the extended Dean−Evans relation[24] to predict and assign the chemical shifts for W_6S_8 clusters with one kind of phosphine ligand and two or more different kinds of L, but the number of possible complexes and isomers is much larger than those examined in this study.

Although a great deal of effort was expended in organizing the enormous amount of ^{31}P NMR data[32] compiled since practical multinuclear NMR spectrometers became available in the 1960s, most revolved around empirically correlating the chemical shifts of substituted phosphines with different substituent groups. The few attempted predictions of chemical shifts for phosphorus-containing inorganic complexes were not accurate enough to be practically useful. The examples presented herein represent a successful empirical correlation of ^{31}P NMR chemical shifts for inorganic complexes, albeit for a limited class of cluster complexes. On the other hand, the numerous analogous examples reported since the discovery of the Dean−Evans relation are mostly various octahedral complexes with $^{19}F^-$ as the NMR nucleus under study,[33] including some very interesting ^{19}F NMR studies of $\{[Mo_6Cl_8]X_{6-n}F_n\}^{2-}$ clusters by Preetz and co-workers.[34] To the best of our knowledge, there were no previous reports of the relation exemplified in ^{31}P NMR chemical shifts. The Dean−Evans relation was also believed to *quantitatively* prove the trans and cis influence of the ligands in the given octahedral complexes.[5] Since trans and cis behavior has been the subject of intense studies and debates,[35] in order to clarify the potential confusion, we use the term trans and cis *"influence"* to describe the thermodynamic phenomenon of a ligand changing the equilibrium ground-state properties of the other ligand(s) in positions trans and cis to it. (The trans and cis "*effects*" are reserved for kinetic effects). This observed cumulative additivity of the C and T constants in eq 3 on phosphine chemical shifts for *octahedral* $W_6S_8L_{6-n}(PR_3)_n$ complexes demonstrates the trans and cis influence of ligands in a broadened sense on *hexanuclear octahedral* metal clusters. Without speculating on the physical and electronic origins of the C and T constants for these clusters, we note that examples presented here contain neutral ligands as opposed to the anionic ligands examined in most previous studies. This could be an interesting topic for theoretical chemists and NMR specialists, including those interested in ab initio calculation of chemical shifts.[36] These C and T constants might be probes for the general properties of Lewis base ligands L, especially those related to the trans and cis influence. However, it is not our intention to experimentally pursue this matter further.

The C and T constants for the same L but different PR_3 ligands are different in Table 2, which will be "explained" in part v after the discussion of the ^{31}P NMR for $W_6S_8(PR_3)_{6-n}(PR'_3)_n$, complexes with two kinds of phosphine ligands.

iv. 2-D ^{31}P NMR Studies of $W_6S_8L_{6-n}(PR_3)_n$ and $W_6S_8(PR_3)_{6-n}(PR'_3)_n$ Complexes. We will digress and examine the simple $W_6S_8(4\text{-tbp})_{6-n}(PEt_3)_n$ (**IIA**) system first. The ^{31}P homonuclear 2-D *J*-resolved (*J*-homo) NMR spectrum can reveal multiplets even if they are overlapping each other in 1-D spectra. For **IIA** (Figure 3A,B), this confirms that the observed splittings are truly due to couplings instead of accidental overlapping. The 2-D homonuclear (P,P)-correlated NMR spectrum (COSY)

(32) Pregosin, P. S.; Kunz, R. W. In *Phosphorus-31 and Carbon-13 NMR of Transition Metal Phosphine Complexes*; NMR Basic Principles and Progress 16; Diehl, P., Fluck, E., Kosfeld, R., Eds.; Springer-Verlag: Berlin, 1979. Pidcock, A. *Adv. Chem. Ser.* **1982**, *196*, 1−22. Minelli, M.; Enemark, J. H.; Brownlee, R. T. C.; O'Connor, M. J.; Wedd, A. G. *Coord. Chem. Rev.* **1985**, *68*, 169−278. Verkade, J. G. *Coord. Chem. Rev.* **1972/1973**, *9*, 1−106. Granger, P. *NMR of Less Common Nuclei*; Academic Press: New York, 1983; pp 385−417, Chapter 13 in ref 41.

(33) There are 91 citations of the original report of the Dean−Evans relation;[24] many of them, if not all, were reviewed in ref 5.

(34) Harder, K.; Peters, G.; Preetz, W. *Z. Anorg. Allg. Chem.* **1991**, *598*, 139−149. Preetz, W.; Harder, K.; Von Schnering, H. G.; Kliche, G.; Peters, K. *J. Alloys Compd.* **1992**, *183*, 413−429. Preetz, W.; Braack, P.; Harder, K.; Peters, G. *Z. Anorg. Allg. Chem.* **1992**, *612*, 7−13. Brueckner, K.; Peters, G.; Preetz, W. *Z. Anorg. Allg. Chem.* **1994**, *620*, 1669−1677.

(35) Coe, B. J.; Glenwright, S. J. *Coord. Chem. Rev.* **2000**, *203*, 5−80. Buchler, J. W.; Kokisch, W.; Smith, P. D. *Struct. Bonding (Berlin)* **1978**, *34*, 79−134. Shustorovich, E. M.; Porai-Koshits, M. A.; Buslaev, Y. A. *Coord. Chem. Rev.* **1975**, *17*, 1−98. Appleton, T. G.; Clark, H. C.; Manzer, L. E. *Coord. Chem. Rev.* **1973**, *10*, 335−422. Hartley, F. R. *Chem. Soc. Rev.* **1973**, *2*, 163−179.

(36) *Modeling NMR Chemical Shifts: Gaining Insights into Structure and Environment.* ACS Symp. Ser. 732; Facelli, J. C., De Dios, A. C., Eds.; American Chemical Society: Washington, DC, 1999. van der Klink, J. J.; Brom, H. B. *Prog. Nucl. Magn. Reson. Spectrosc.* **2000**, *36*, 89−201.

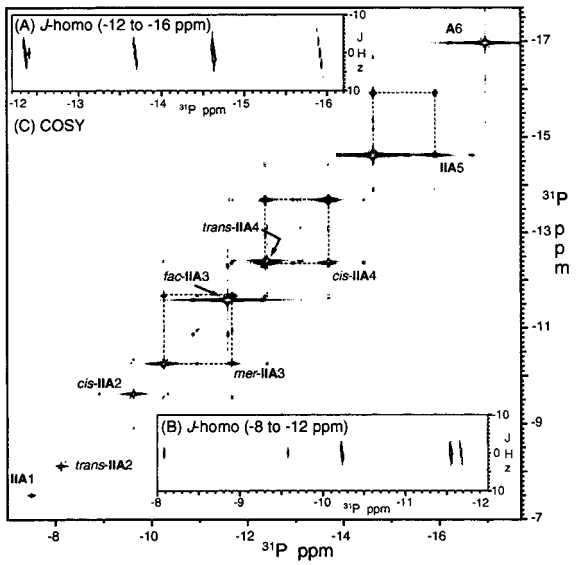

Figure 3. 2-D $^{31}P\{^1H\}$ NMR spectra for a mixture of $W_6S_8(4\text{-tbp})_{6-n}(PEt_3)_n$ ($n = 1-6$) complexes: (A and B) *J*-homo; (C) COSY.

(Figure 3C) reveals the couplings between different ^{31}P nuclei when the off-diagonal cross-peaks form a square with the coupling diagonal peaks. Due to the high solubility of $W_6S_8(4\text{-tbp})_{6-n}(PEt_3)_n$, the signals in this COSY are so intense that the cross-peaks between some satellite peaks are also visible, directly and conclusively confirming the speculation that the satellites splittings originate from ^{31}P nuclei on ^{183}W cluster isotopomers.[15]

Merely serving as reaffirmation for $W_6S_8L_{6-n}(PR_3)_n$ systems, 2-D NMR is indispensable for deciphering mixtures of $W_6S_8(PR_3)_{6-n}(PR'_3)_n$ complexes because the now 24 peaks couple to each other extensively and they often overlap. In the 1-D ^{31}P NMR spectrum displayed in Figure 4A (top) for $W_6S_8(PEt_3)_{6-n}(P^nBu_3)_n$ (**AB**) complexes, two groups of "messy" peaks appear at around δ −17 and −24, corresponding to the two kinds of bound phosphines on the clusters, PEt_3 (**A**) and P^nBu_3 (**B**), respectively. (The chemical shift for $W_6S_8(PEt_3)_6$ is δ −16.97, and that for $W_6S_8(P^nBu_3)_6$ is δ −24.44.[31]) Shown in Figure 4C (bottom), the *J*-homo NMR resolved a total of 12 overlapping multiplets, ranging from singlet to septet, for the P^nBu_3 side (around δ −24) of the spectrum, just as expected for a complete series. From the predicted coupling schemes for complexes in the **AB** series that are listed in Table 3, P^nBu_3 on *trans*-**AB**4 (i.e. *trans*-$W_6S_8(PEt_3)_2(P^nBu_3)_4$; "4" denotes the number of P^nBu_3 groups bound to the cluster) and **AB**5 should give the only two triplets (δ −24.6 and −24.75) and *fac*-**AB**3 should give the only quartet (δ −24.72) for the P^nBu_3 side. The *J*-homo for the PEt_3 side (available in the Supporting Information) is still quite congested, but since most complexes (except for the known terminal members) in the series have signals in both regions, this does not compromise their identification. The COSY spectrum (Figure 4B with the interesting regions expanded and placed in the center as B1−B4) contains a plethora of information with the cross-peaks between both P^nBu_3 ligands ("intraligand") and two phosphines PEt_3 and P^nBu_3 ("interligand"). Within the PBu_3 region (Figure 4B2), three apparent pairs of "intraligand" couplings are highlighted with dashed-line squares and can be assigned to **AB**5, *cis*-**AB**4, and *mer*-3**AB**. All PBu_3 peaks but one ($W_6S_8(P^nBu_3)_6$ at δ −24.44)

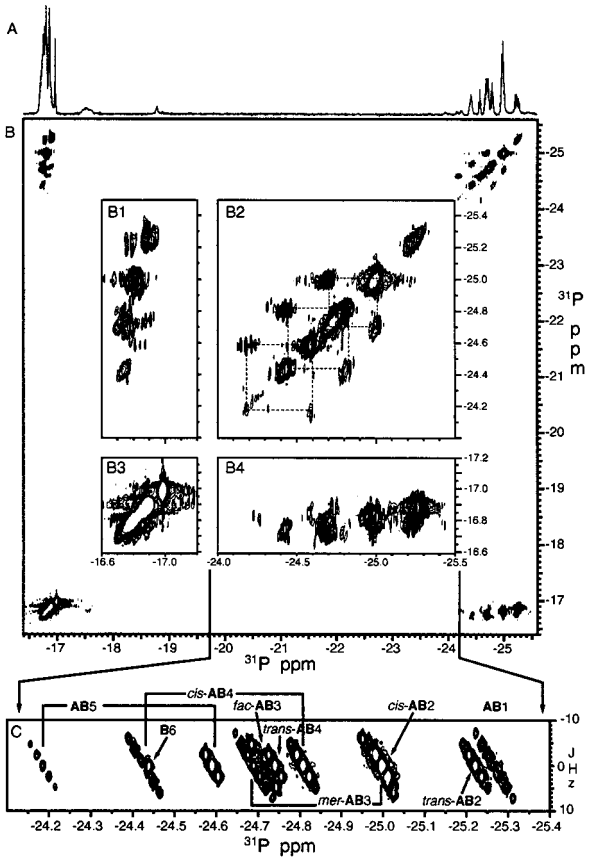

Figure 4. $^{31}P\{^1H\}$ NMR spectra for a mixture of $W_6S_8(PEt_3)_{6-n}(P^nBu_3)_n$ ($n = 0-6$) complexes: (A) 1-D; (B) COSY (the expanded regions of interest (B1−B4) are placed in the center of the panel); (C) *J*-homo of the P^nBu_3 region (δ −24.0 to −25.4).

have "interligand" coupling, and among them those four peaks from complexes *mer*-**AB**3, *cis*-**AB**2, and **AB**1 (the three "intraligand" coupling pairs for PEt_3 side) should have two "interligand" coupling interactions. Also, a controlled reaction of $W_6S_8(P^nBu_3)_6$[31] with less than 1 equiv of PEt_3 yielded primarily one product, **AB**5, or **AB**1 if the converse was carried out. A combination of the above analyses leads to complete identification of all 10 species present in the mixture and all 12 NMR peaks in the P^nBu_3 region, as labeled in Figure 4C.

It is apparent from the assigned P^nBu_3 region of the spectrum that the chemical shifts still progress regularly—but now from right (upfield) to left (downfield) as more P^nBu_3 is added and the pairs of coupled peaks intermingle. Fitting with eq 3 yielded $C = -0.24 \pm 0.01$ and $T = 0.09 \pm 0.04$. The significance is that phosphines influence each other, though such influence is not reciprocal (the PEt_3 region of the spectrum is not as spread out as the P^nBu_3 portion). Due to the sensitivity of the NMR spectrometer, COSY spectra for the less soluble $W_6S_8(PEt_3)_{6-n}(PCy_3)_n$ (**AZ**) complexes are not as conclusive. Since the interpretation process is similar, those spectra are included in the Supporting Information.

v. Expanding the Dean−Evans Relation. From the discussion of the above two sections, it becomes apparent that the Dean−Evans relation needs to be expanded to account for this added dimension of different phosphine ligands, which was not of concern at all in the original Dean−Evans relation[24] since the anionic ligand (F^-) is monatomic. If one considers the additive nature of the Dean−Evans equation, one realizes that

Table 3. Predicted Coupling Schemes of $W_6S_8(PEt_3)_{6-n}(P^nBu_3)_n$ ($n = 1 - 5$; AB) Complexes

n	name[a]	Structure[b] diagram	peak ratios multiplicity[c]
1	**AB1**	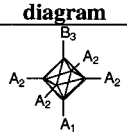	$A_1:A_2:B_3$ 1 : 4 : 1 sextet : triplet : **sextet**
2	*trans*-**AB2**	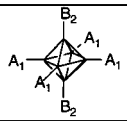	$A_1:B_2$ 2 : 1 triplet : **quintet**
	cis-**AB2**	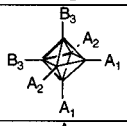	$A_1:A_2:B_3$ 1 : 1 : 1 quintet : quintet : **quintet**
3	*mer*-**AB3**	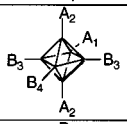	$A_1:A_2:B_3:B_4$ 1 : 2 : 2 : 1 septet: sextet: **sextet: septet**
	fac-**AB3**	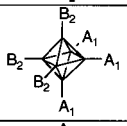	$A_1:B_2$ 1 : 1 quartet : **quartet**
4	*trans*-**AB4**	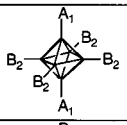	$A_1:B_2$ 1 : 2 quintet : **triplet**
	cis-**AB4**	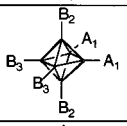	$A_1:B_2:B_3$ 1 : 1 : 1 quintet : **quintet : quintet**
5	**AB5**	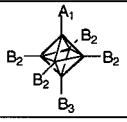	$A_1:B_2:B_3$ 1 : 4 : 1 sextet : **triplet : sextet**

[a] The number *n* indicates the number of P^nBu_3 (**B**) ligands. [b] The octahedron represents the W_6S_8 cluster; A and B are PEt_3 and P^nBu_3 ligands, respectively. [c] Multiplets in boldface are those from P^nBu_3 (**B**) ligands. There are uncertainties about those splitting by both PEt_3 and P^nBu_3 ligands across the cluster axis, depending upon their coupling constants (*J*) to the P under question.

a more fundamental way of summing up the influence in a $W_6S_8L_{6-n}(PR_3)_n$ complex should include not only the influence from ligand L but also that from the rest of the PR_3 ligands:

$$\delta(^{31}\mathrm{P}) = \delta_{\mathrm{ref}} + pC_L + qT_{\mathrm{L}} + PC_P + QT_{\mathrm{P}} \qquad (4)$$

where $\delta(^{31}\mathrm{P})$, δ_{ref}, p, and q are as defined in eq 3, P is the number of phosphine ligands (PR_3) in positions cis to the P atom under consideration (0−4), Q is the number of phosphine ligands (PR_3) in positions trans to the P atom under consideration (0, 1), and C_{P} and T_{P} constants are analogous constants except for the fact that they are for phosphine ligand PR_3 and thus are denoted with the subscript "P" to differentiate from those for ligand L (C_{L} and T_{L}). Each time a non-phosphine ligand L is added to $W_6S_8L_{6-n}(PR_3)_n$, a phosphine ligand PR_3 must be taken off. Since $p + P = 4$ and $q + Q = 1$, $P = 4 - p$ and $Q = 1 - q$, and eq 4 becomes

$$\begin{aligned}\delta(^{31}\mathrm{P}) &= \delta_{\mathrm{ref}} + pC_L + qT_{\mathrm{L}} - pC_P - qT_{\mathrm{P}} + 4C_P + T_{\mathrm{P}} \\ &= \delta_{\mathrm{ref}} + 4C_P + T_{\mathrm{P}} + p(C_L - C_P) + q(T_{\mathrm{L}} - T_{\mathrm{P}}) \qquad (5)\end{aligned}$$

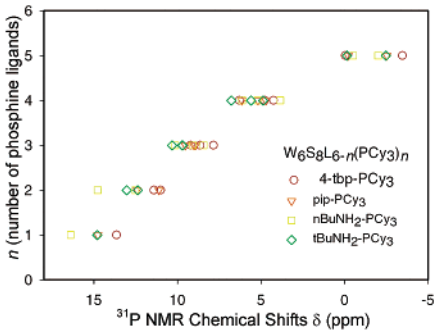

Figure 5. Attempted Dean−Evans plot (n vs $\delta(^{31}\mathrm{P})$) for $W_6S_8L_{6-n}(PCy_3)_n$ clusters ($n = 1-5$).

If we compare eq 5 with the observed eq 3, it is easy to see that

$$\begin{aligned}\delta'_{\mathrm{ref}} &= \delta_{\mathrm{ref}} + 4C_P + T_{\mathrm{P}} \\ C &= C_{\mathrm{L}} - C_{\mathrm{P}} \\ T &= T_{\mathrm{L}} - T_{\mathrm{P}} \qquad (6)\end{aligned}$$

i.e., the experimentally observed C and T constants are really the difference between the "true" C and T constants for the two types of ligands. Therefore, the differences in the C and T constants for the same ligand L but different phosphines (see Table 2) reflect the empirical differences between the phosphines. Although we cannot identify any consistent trends with the limited number of examples we have studied so far, this expansion of the original Dean−Evans relation theoretically allows for the observed differences seen in various families of $W_6S_8L_{6-n}(PR_3)_n$ and $W_6S_8(PR_3)_{6-n}(PR'_3)_n$.

vi. Exceptions to the Dean−Evans Relation. Fits of the Dean−Evans equation fail when bulky ligands such as tricyclohexylphosphine (PCy_3) and triphenylphosphine (PPh_3) are attached to W_6S_8. As shown in Figure 5, though the ordering of the chemical shifts for $W_6S_8L_{6-n}(PCy_3)_n$ ($n = 0-5$) complexes still holds, the chemical shifts of those phosphine-rich complexes ($n = 4$, 5) deviate significantly toward the upfield direction from the extrapolated straight lines of the phosphine-poor complexes ($n = 1-3$). The data from the rest of the undisplayed "deviant" systems behave much in the same manner, but to a different degree. This breakdown of the Dean−Evans relation can be explained by sterics. Tricyclohexylphosphine and triphenylphosphine are among the most sterically demanding phosphines by cone angle criteria,[37] as confirmed by our crystallographic study of the homoleptic clusters.[15,31] It was well-documented in the literature that confined environments would change the angles between the three substituent groups of the phosphine ligands and thus change the bonding characteristics of P−M bonds and finally the chemical shifts of the phosphine under question.[37] Although the fact that the phosphine-rich cluster complexes deviate more significantly from the Dean−Evans prediction implies the steric hindrance might be between the axial ligands, we cannot exclude the role of steric repulsion between these bulky ligands and the cluster core. In any case, if we accept the general validity of the Dean−Evans relation, a Dean−Evans plot can be a convenient way of probing any possible steric effects for the ligands of interest.

(37) Tolman, C. A. *Chem. Rev.* **1977**, *77*, 313−348. Muller, T. E.; Mingos, D. M. P. *Transition Met. Chem.* **1995**, *20*, 533−539.

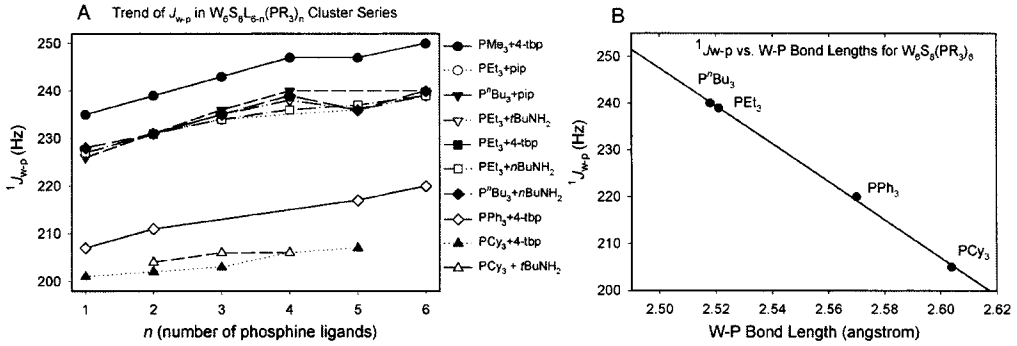

Figure 6. (A) Plot of the W−P coupling constants ($^1J_{W-P}$) vs the number of phosphine ligands (n) for selected $W_6S_8L_{6-n}(PR_3)_n$ ($n = 1-6$) complexes. (B) Plot of the W−P coupling constants ($^1J_{W-P}$) from $W_6S_8(PR_3)_6$ clusters vs the average W−P bond lengths from the $W_6S_8(PR_3)_6$ structures. The $^1J_{W-P}$ value for the doublet from W_6S_8(4-tbp)$(PCy_3)_5$ is used when R = Cy.

vii. Satellites and W−P Coupling Constants. When ^{31}P NMR spectra are sufficiently intense and the main resonance does not interfere with other satellites, the W−P coupling constants ($^1J_{W-P}$) for some complexes can be determined. All available $^1J_{W-P}$ data are plotted against the number of the phosphine ligands (n) in Figure 6A. There is a subtle but clear trend of $^1J_{W-P}$ increasing as more phosphine ligands are attached. This is perhaps another manifestation of the accumulative influence of the ligands on ground-state properties of the cluster complexes, though it is not as sensitive as the chemical shifts. Also in Figure 6B, the coupling constants ($^1J_{W-P}$) for $W_6S_8(PR_3)_6$ (the $^1J_{W-P}$ for the doublet from W_6S_8(4-tbp)$(PCy_3)_5$ is used when R = Cy as $W_6S_8(PCy_3)_6$ is insoluble in common NMR solvents) are plotted against the average W−P bond lengths from the known $W_6S_8(PR_3)_6$ clusters.[31] There appears to be an excellent linear correlation between the coupling constants and the bond lengths.[38] Combining both figures, it is reasonable to believe that W−P bond lengths in general decrease slightly as more and more phosphine ligands are bound to the clusters.

B. Cluster Distributions and Separation Attempts. Among the heteroleptic complexes formed in reaction 1, the *trans*-P2 and *trans*-P4 complexes are specifically desired to prepare two- and one-dimensional compounds when ditopic ligands are used to link clusters into coordination solids. However, it was suspected on the basis of the complicated ^{1}H NMR obtained before this study, and now definitely confirmed with many ^{31}P NMR spectra, that reacting $W_6S_8L_6$ complexes with less than 6 equiv of PR_3 produces every possible $W_6S_8L_{6-n}(PR_3)_n$ ($n = 0-6$) complex in the series:

$$W_6S_8L_6 + xPR_3 \rightarrow W_6S_8L_{6-n}(PR_3)_n + nL + (x-n)PR_3 \quad x < 6 \quad (7)$$

This facilitates the sample preparation for this study but undermines the efforts to isolate specific complexes. In a *statistical* model, the probability, $P(n)$, of finding an *octahedral* $W_6S_8L_{6-n}(PR_3)_n$ complex with a given number of new ligands (n) is given by the binomial distribution

$$P(n) = \frac{6!}{(6-n)!n!}p^n(1-p)^{6-n} \quad n = 0-6 \quad (8)$$

where p is the probability of finding a phosphine ligand bound to a W atom. When both ligands have the same ligand binding free energy ($\Delta G(PR_3) = \Delta G(L)$) to the W_6S_8 cluster, p is just the *nominal* mole fraction of the new ligand; i.e., $p = x/(6 + x)$. Figure 7A shows the general equilibrium diagram drawn using eq 8. When the two ligands have different binding free energies to W_6S_8, the probability p used in eq 8 should be

$$p = \frac{fe^{-\Delta G/RT}}{(1-f) + fe^{-\Delta G/RT}} \quad (9)$$

where the binding free energy difference $\Delta G = \Delta G(PR_3) - \Delta G(L)$ and where f is the mole fraction of free PR_3 in the ligand bath. Such an equation is valid when the number of moles of each ligand in the bath is much larger than the number of moles of cluster in equilibrium with the bath. It is evident that as ΔG becomes more negative, the probability of PR_3 binding to a W site increases. In our experiments, however, the ligand bath is small and f is not equal to the initial mole fraction. However, it is clear even in this case that as ΔG becomes more negative, more phosphines will be bound to the cluster than that predicted by eq 8 with $p = x/(6 + x)$. Also, if x is less than 6 and ΔG becomes more negative, then $p = x/6$. The equilibrium diagram for this extreme case is shown in Figure 7B. We would expect that the experimental results would fall between these two extremes, assuming each ligand binding free energy is independent of the number and configuration of all the other ligands. The experimental equilibrium distributions were computed with ^{31}P NMR signal intensities for the W_6S_8(4-tbp)$_{6-n}(PEt_3)_n$ (**IIA**) cluster series at two different values of x (2.6 and 4.3 for Figure 7C,D, respectively) and shown in comparison with the predictions from these two extremes.[39] At both values of x, the number of phosphines bound to W_6S_8 is strongly biased to $n = 5, 6$; at lower values of n the fractions of observed complexes are somewhat decreased, as they must be by mass balance. This observation suggests there is a significant cis and/or trans influence of the ligand binding energy. This effect is not included in the statistical model above (eqs 8 and 9). Although the cis/trans or mer/fac ratios between the three pairs of

(38) As opposed to some rather nonlinear correlation of M−P coupling vs bond lengths found in the literatures such as: Mason, R.; Meek, D. W. *Angew. Chem.* **1978**, *90*, 195−206. This correlation is likely due to the small range of values for the case at hand.

(39) The successive equilibrium constants are difficult to calculate, as the small amounts of free phosphines found in most reactions cannot be accurately measured. The distributions are reported with the mole equivalents of phosphine (x) determined with quantitative ^{1}H NMR. Since $W_6S_8L_6$ is not observable in ^{31}P NMR, both experimental and theoretical distributions are renormalized to the observable complexes ($n = 1-6$).

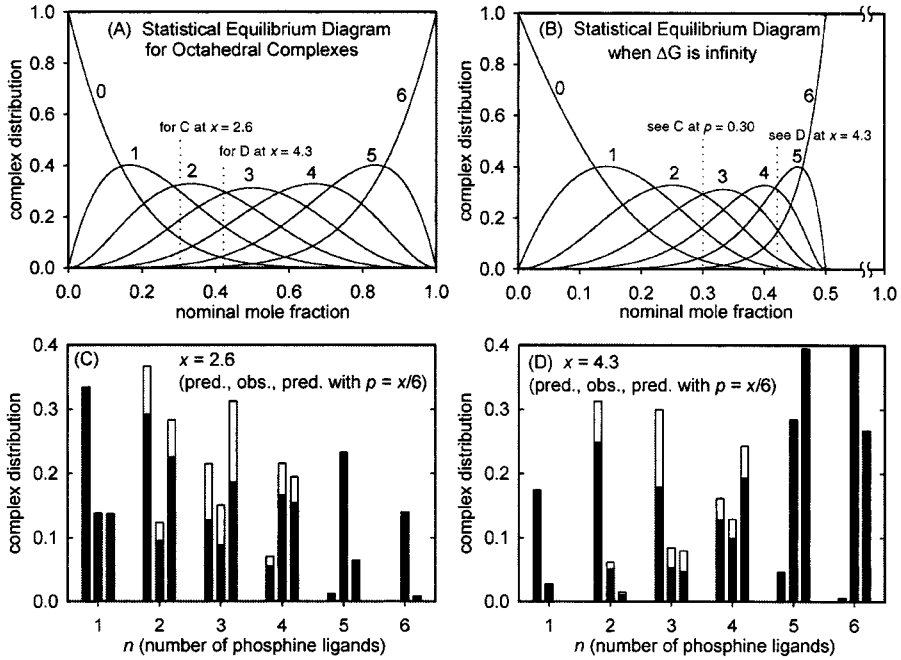

Figure 7. (A) Equilibrium diagram for a series of octahedral complexes based on statistical binomial distribution. (B) The same diagram as (A), except with one ligand strongly favored over the other ($\Delta G \rightarrow -\infty$ and $x < 6$). (C and D) Observed distributions of $W_6S_8(4\text{-tbp})_{6-n}(PEt_3)_n$ ($n = 1-6$) complexes determined by ^{31}P NMR (the middle bars in each group) vs the statistical predictions from (A) (left bars) and (B) (right bars) at phosphine equivalents (x) of 2.6 (C) and 4.3 (D). The stacked empty and filled bars for $n = 2-4$ represent the proportions of the trans/cis and fac/mer stereoisomers, respectively.

stereoisomers should not be affected by the difference of binding free energy between ligands, the experimental values (shown with empty and solid bars in Figure 7C,D) are often slightly larger than the theoretical values of 4 and 1.5 (experimental values range from 3.5 to 5.6 for cis/trans and 1.5 to 1.9 for mer/fac for these two cases), making the desired *trans*-**IIA**2 and *trans*-**IIA**4 complexes even less accessible. This again is the result of cis and/or trans interactions. These stereoisomeric ratios are even larger for the heteroleptic clusters with bulky PCy_3 and PPh_3 ligands. However, this additional discrepancy is attributed to sterics, as previously discussed for the $W_6S_8(4\text{-tbp})_{6-n}(PCy_3)_n$ clusters.[15] The distributions described there can be similarly reproduced in the $W_6S_8(\text{piperidine})_{6-n}(PCy_3)_n$ series, confirming our steric arguments. In summary, except for the possibility of somewhat *stereoselective* cluster preparation with bulky ligands,[15] the naïve hope of preparing a specific cluster in significant yield by varying the reaction stoichiometry (x) is generally impractical. If specific isomers are to be prepared, some separation scheme must be worked out.

A note of caution is necessary, since the statement above is based on equilibrium behavior. In fact, an exceptional case is the seemingly stepwise reactions of $[Re_6Q_8X_6]^{4-}$ (Q = S, Se; X = Br, I) with PEt_3 by Zheng et al.,[12] where the kinetics appear to be slow enough to allow the capture of different reaction intermediates $[Re_6Q_8X_{6-n}(PEt_3)_n]^{4-n}$ by varying reaction times and stoichiometry. However, such evolution of W_6S_8 complexes was not observed at any temperature, probably due to the much faster reaction kinetics than for $\{Re_6Q_8\}^{2+}$ clusters. Intermediate times reactions for W_6S_8 (observed with ^{31}P NMR) produced many "evenly" distributed species similar to the general picture of the equilibrated mixtures but with some unreacted phosphines.

The efforts made to separate the $W_6S_8(4\text{-tbp})_{6-n}(PEt_3)_n$ complexes have not been very successful so far. As shown by ^{31}P NMR, solvents that dissolve the terminal homoleptic clusters, such as benzene and THF, are even better solvents for the heteroleptic complexes. Many solvents that do not dissolve the terminal complexes, such as diethyl ether, acetonitrile, and heptane, can dissolve the heteroleptic clusters to different extents: acetonitrile is a better solvent for the phosphine-poor complexes, heptane is better for the phosphine-rich complexes and diethyl ether rather uniformly solubilizes across the series. Using such differences, some degree of enrichments could be achieved, but not isolation of a single isomer. After all, the physical properties of $W_6S_8(4\text{-tbp})_{6-n}(PEt_3)_n$ are quite similar, as the polarity differentiation of these neutral complexes is minute. This is in marked contrast to the different charges and counterions exploited in the remarkable chromatographic separation of $[Re_6Q_8X_{6-n}(PEt_3)_n]^{4-n}$.[12,14] The chromatography of the $W_6S_8(4\text{-tbp})_{6-n}(PEt_3)_n$ cluster mixtures was also plagued by decomposition on silica gel or Florisil gel, either due to the acidity or perhaps due to oxidation.[40] Reproducible separation on a large scale remains a significant challenge.

C. Crystal Structures. Since there were always microcrystalline precipitates that are impossible to analyze with X-ray diffraction, the species observed were those most easily crystallized from a particular mixture. This situation illustrates the very point that analytical tools such as those developed herein are sorely needed for cluster research, because one cannot depend on X-ray crystallographic analysis of rare crystals. Though repeatable, using crystallization to isolate a specific isomer is quite tedious, as further mechanical separation is needed. Also, if the desired isomer does not crystallize, you are out of luck.

Nevertheless, crystallographic analysis for the carefully selected precious crystals confirmed the identity of several cluster complexes among those expected by NMR spectroscopy. These are shown in Figure 8. All molecular structures share the same familiar octahedral W_6S_8 core and have mixed ligands, which causes the low crystallographic and metric symmetry.

(40) Hill, L. I.; Jin, S.; Zhou, R.; Venkataraman, D.; DiSalvo, F. J. *Inorg. Chem.* **2001**, *40*, 2660−2665.

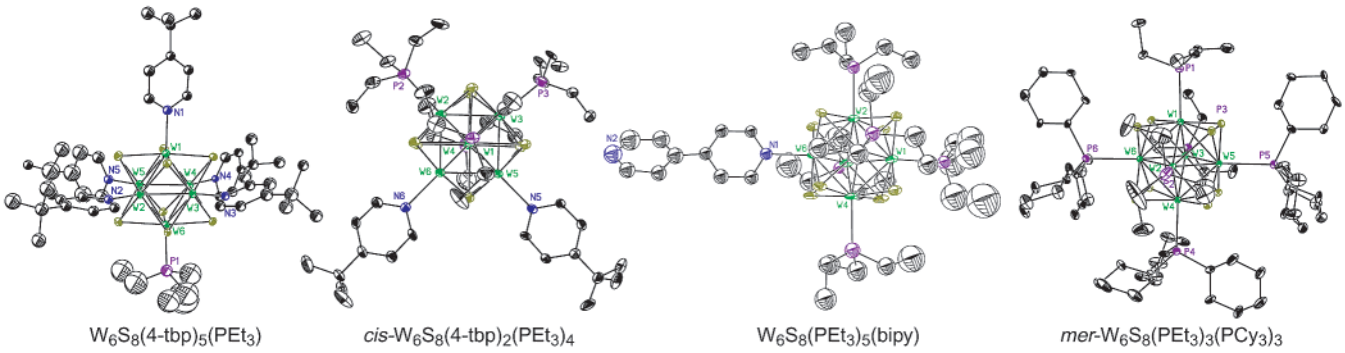

Figure 8. Molecular structures of $W_6S_8(4\text{-tbp})_5(PEt_3)$, *cis*-$W_6S_8(4\text{-tbp})_2(PEt_3)_4$, $W_6S_8(PEt_3)_5(bipy)$, and *mer*-$W_6S_8(PEt_3)_3(PCy_3)_3$ clusters with a partial labeling scheme and no H atoms. The thermal ellipsoids are at the 30% probability level.

Table 4. Selected Interatomic Distances (Å) and Bond Angles (deg) for Clusters **1**−**4**[a]

	1	2	3[e]	4
W−W	2.6468(12)−2.6804(11)	2.6463(5)−2.6892(5)	2.657(2)−2.692(2)	2.6653(7)−2.6955(6)
mean[a]	2.663(12)	2.670(12)	2.683(8)	2.683(8)
δ_{W-W}[b]	0.044	0.043	0.035	0.030
W−S	2.452 (5)−2.482(5)	2.4494(19)−2.4689(19)	2.428(9)−2.481(8)	2.432(3)−2.467(3)
mean[a]	2.465(8)	2.457(6)	2.456(12)	2.447(9)
δ_{W-S}[b]	0.030	0.020	0.053	0.035
W−W−W[c]	89.32(4)−90.74(4)	89.232(15)−90.523(16)	89.25(7)−90.54(7)	89.36(2)−90.66(2)
δ_{w-w-w}[b]	1.42	1.29	1.29	1.30
W−W−W[d]	59.20(3)−60.68(3)	59.171(13)−60.765(13)	59.38(5)−60.59(5)	59.36(2)−60.54(2)
δ_{w-w-w}[b]	1.48	1.592	1.21	1.18
W−N	2.22(2), 2.258(14), 2.221(14), 2.26(2), 2.27(2) (trans to P)	2.263(7), 2.257(6)	2.25(2), 2.31(2)	2.534(3), 2.530(4), 2.532(3) (W−PEt_3)
mean[a]	2.25(2)	2.260(7)	2.28(3)	2.532(4)
W−P	2.524(7)	cis, 2.522(2), 2.543(2); trans, 2.518(2), 2.509(2)	2.502(11) −2.564(12)	2.595(3), 2.598(3), 2.615(3) (W−PCy_3)
mean[a]		2.523(12)	2.525(18)	2.603(15)

[a] Followed by standard deviations (σ) of the group of bond lengths in the parentheses. $\sigma = \{\sum(d_j - d_m)^2/n\}^{1/2}$. [b] Maximum deviations. [c] Within equatorial squares. The mean W−W−W angles within the equatorial squares are automatically 90° if the clusters have inversion centers. [d] Within triangular faces. The mean angles are 60° by geometry. [e] There are two independent clusters in structure **3**. The values shown are for both.

Selected bond lengths and angles are presented in Table 4. The variations on the bond lengths and angles within each cluster are rather large (compared with the variations for homoleptic $W_6S_8L_6$ complexes), even though the bond lengths and angles are close to the values from the related $W_6S_8L_6$ clusters.[31] The W−W bond lengths observed in the $W_6S_8(4\text{-tbp})_{6-n}(PEt_3)_n$ structures (**1** and **2**) range from 2.6463(5) to 2.6892(5) Å, compared with the average W−W bond lengths in the two terminal complexes, 2.662 Å ($W_6S_8(4\text{-tbp})_6$) and 2.680 Å ($W_6S_8(PEt_3)_6$).[31] The W−L bond lengths are slightly longer than the average W−L bond lengths in the terminal $W_6S_8(4\text{-tbp})_6$ and $W_6S_8(PEt_3)_6$ complexes.[31] Given the observed trend in W−P coupling constants ($^1J_{W-P}$) (part vii of section A), these changes in bond lengths may be subtle reflections of the electronic changes that occur on the stepwise substitution of the ligands, although such changes are much less sensitive than those observed in NMR spectroscopy.

Summary and Outlook

This and previous work[15] make the following clear.

(1) In situ identification of many $W_6S_8L_{6-n}(PR_3)_n$ clusters by ^{31}P NMR is possible due to an uncommon long-range P−P *J* coupling.

(2) For the first time, the Dean−Evans relation for ^{31}P NMR chemical shifts is shown to apply to the $W_6S_8L_{6-n}(PR_3)_n$ clusters. The Dean−Evans relation demonstrates the trans and cis influence of the ligands on hexanuclear clusters, predicts the chemical shifts, and helps spectroscopic assignments. When it fails with bulky ligands, ^{31}P NMR can be used as a "sterics indicator".

(3) With the help of 2-D ^{31}P NMR spectroscopy (*J*-homo and COSY), even the NMR of $W_6S_8(PR_3)_{6-n}(PR'_3)_n$ ($n = 0-6$) complex mixtures can be unequivocally interpreted.

(4) The Dean−Evans relation is expanded to account for different phosphine ligands.

(5) Substitution reactions of $W_6S_8L_6$ with less than 6 equiv of phosphine ligands were found by ^{31}P NMR to produce the entire series of cluster complexes, but separation is needed if specific complex(es) is (are) desired.

In summary, ^{31}P NMR and other NMR techniques, combined with Dean−Evans relations, are invaluable analytical tools in the study of molecular W_6S_8 cluster chemistry. Furthermore, there must be analogous relations exemplified in various NMR nuclei to be discovered among the many other diamagnetic *octahedral clusters* of both structural types (M_6X_8 and M_6X_{12}).[2−9] One has reason to believe that the same physical effects ought to be observable in these clusters, if the ligands are convenient to observe by NMR (such as ^{31}P, ^{19}F, and ^1H and perhaps also enriched ^{13}C),[41] and are sufficiently sensitive to their environments.[42] The progression of symmetry with stepwise change of the building units on a highly *symmetrical octahedral cluster*

(41) *Multinuclear NMR*; Mason, J., Ed.; Plenum Press: New York, 1987.
(42) We have also preliminarily observed the Dean−Evans relations in ^{31}P chemical shifts for $Mo_6S_8L_{6-n}(PR_3)_n$ and $[W_6Cl_8Cl_{6-n}(PR_3)_n]^{n-2}$ complexes.

presents not only rich opportunities but also tremendous challenges for analyzing the many resulting compounds.[5,11−16,43] As an interesting example, the "disordered" $[Re_6Te_{8-n}Se_n(CN)_n]^{4-}$ cluster complexes,[44] which have two chalcogens as the eight face-capping inner ligands, can have up to 22 complexes that could not be distinguished by X-ray crystallography, and 55 chemical shifts are observed in a remarkably busy but regular ^{125}Te NMR spectrum. Perhaps a three-parameter relation that accounts for the influences of Se atoms in position next to, face diagonal to, and body diagonal to the Te atom under question could predict these ^{125}Te chemical shifts in a manner similar to the Dean−Evans relation and, therefore, could greatly simplify the spectroscopic assignments. From an even broader perspective, analogues of the Dean−Evans relation might even exist for the chemical shifts of the ligands of high-symmetry nanoclusters,[45] when the clusters have uniform size and composition. More parameters and higher sensitivity are certainly needed to detect the *subtle* changes on a *giant* nanocluster, but such relations, if they exist, would render unprecedented analytical ability to such research. Werner established the coordination chemistry of single *octahedral metal complexes* as we know today without X-ray crystallography and spectroscopy, but it was when these modern techniques became available that this chemistry really blossomed. Hopefully, the chemistry of *metal clusters* will benefit from this and other[13,44,46−47] NMR spectroscopic studies.

Acknowledgment. This work was supported by the Department of Energy (Grant No. DE-FG02-87ER45298). The CCMR (the Cornell Center for Materials Research) REU (Research Experience for Undergraduate) program is thanked for the support of J.A. during the summer of 2000. Experimental assistance from our colleagues Ellen Scheuer and Ran Zhou is also acknowledged.

Supporting Information Available: Tables of the compiled ^{31}P NMR chemical shifts for all of the systems investigated and of T_1 relaxation times for ^{31}P nuclei in $W_6S_8(4\text{-tbp})_{6-n}(PR_3)_n$ clusters, figures giving more 2-D $^{31}P\{^1H\}$ NMR spectra of $W_6S_8(PR_3)_{6-n}(PR'_3)_n$ complex mixtures, X-ray crystallographic files in CIF format for the structure determinations of $W_6S_8(4\text{-tbp})_5(PEt_3)\cdot 3C_6H_6$ (**1**), *cis*-$W_6S_8(4\text{-tbp})_2(PEt_3)_4$ (**2**), $W_6S_8(PEt_3)_5(bipy)$ (**3**), and *mer*-$W_6S_8(PEt_3)_3(PCy_3)_3\cdot 2C_6D_6$ (**4**), and the details from SigmaPlot 2000 software for the fitting of the ^{31}P NMR chemical shifts. This material is available free of charge via the Internet at http://pubs.acs.org.

JA0257873

(43) Tulsky, E. G.; Long, J. R. *Inorg. Chem.* **2001**, *40*, 6990−7002.
(44) Mironov, Y. V.; Cody, J. A.; Albrecht-Schmitt, T. E.; Ibers, J. A. *J. Am. Chem. Soc.* **1997**, *119*, 493−498.
(45) Tran, N. T.; Powell, D. R.; Dahl, L. F. *Angew. Chem., Int. Ed.* **2000**, *39*, 4121−4125. Schmid, G. *Struct. Bonding (Berlin)* **1985**, *62*, 51−85. *Clusters and Colloids. From Theory to Application;* Schmid, G., Ed.; VCH: Weinheim, Germany, 1994.
(46) Ebihara, M.; Toriumi, K.; Saito, K. *Inorg. Chem.* **1988**, *27*, 13−18.
(47) Weinert, C. S.; Stern, C. L.; Shriver, D. F. *Inorg. Chim. Acta* **2000**, *307*, 139−143.